ChemComm

COMMUNICATION

View Article Online
View Journal | View Issue

Cite this: *Chem. Commun.*, 2015, 51, 8480

Received 17th March 2015,
Accepted 10th April 2015

DOI: 10.1039/c5cc02233a

www.rsc.org/chemcomm

Tunnel-structured $Na_{0.54}Mn_{0.50}Ti_{0.51}O_2$ and $Na_{0.54}Mn_{0.50}Ti_{0.51}O_2$/C nanorods as advanced cathode materials for sodium-ion batteries†

Xiaolei Jiang,[a] Shuo Liu,[a] Huayun Xu,[a] Liang Chen,[a] Jian Yang*[a] and Yitai Qian[ab]

Tunnel-structured $Na_{0.54}Mn_{0.50}Ti_{0.51}O_2$ nanorods have been synthesized by a facile molten salt method. These nanorods are grown in the direction normal to the sodium-ion tunnels, greatly shortening the diffusion distance of sodium ions and benefiting the transfer kinetics. Thus, the nanorods show significant enhancements in terms of reversible capacity, cycling stability and rate capability. The electrochemical performance could be further promoted *via* carbon coating to ~122 mA h g^{-1} after 150 cycles at 0.2 C or ~85 mA h g^{-1} after 400 cycles at 1 C.

Rechargeable lithium ion batteries have been widely applied in various portable electronic devices and hybrid vehicles due to their high energy density. However, high cost and safety concerns in some extreme environments constraint their utilization.[1] Therefore, Na-ion batteries (SIBs) are regarded as promising alternatives to the well-developed Li-ion batteries,[2–6] due to their low cost, good and safe handling and environmental friendliness. So far, most reports for cathode materials are focused on layer-structured transitional metal oxides. A typical example of this trend is the case of TiO_6-based cathode materials.[7–9] The non-toxic and cheap characteristics of titanium, with their fair electrochemical properties, make this family quite attractive.

In spite of this, it is necessary to explore other structures, because they might show promising potential as cathode materials for SIBs. This has been validated by one recent report on $Na_{0.61}Mn_{0.52}Ti_{0.48}O_2$, a tunnel structural analogue to $Na_4Mn_4Ti_5O_{18}$.[10] The highly aggregated $Na_{0.61}Mn_{0.52}Ti_{0.48}O_2$ powders obtained by a solid-state reaction presented a specific capacity of 86 mA h g^{-1} after 100 cycles at a current density of 20 mA g^{-1}. Although this electrochemical performance is not at the top of the reported list, it shows the opportunities to achieve the good sodium-storage performance *via* non-layered structures. Since only sodium ions in the S-shape tunnels of $Na_4Mn_4Ti_5O_{18}$ are mobile,[11–13] the rational design and delicate control of the tunnel length and size of the cathode material become extremely important, which is well demonstrated for $LiFePO_4$ in lithium ion batteries (LIBs).[14–16] However, it has not been reported for this structure before.

Herein, the tunnel-structured nanorods of $Na_{0.54}Mn_{0.50}Ti_{0.51}O_2$ are synthesized by a molten salt method for the first time. The nanorods do not simply assemble nanoscale size and well-defined shape within one particle, but have the length of the sodium-ion tunnels on the nanoscale. This kind of control would shorten the sodium-ion diffusion distance, facilitate the transfer kinetics and improve its electrochemical performance, which is supported by reversible capacity and rate capability. The performance could be further promoted *via* carbon coating to ~122 mA h g^{-1} after 150 cycles at 0.2 C, or ~85 mA h g^{-1} after 400 cycles at 1 C, much higher than those in previous reports.

$Na_{0.54}Mn_{0.50}Ti_{0.51}O_2$ nanorods were synthesized by a modified molten-salt process,[17] in which CH_3COONa, $Mn(CH_3COO)_2$, and TiO_2 reacted at 800 °C in a mixture of molten NaCl–KCl (see ESI†). Fig. 1 shows the XRD pattern of the resultant product. The peaks can be indexed on the basis of an orthorhombic structure with a space group of Pbam ($Na_4Mn_4Ti_5O_{18}$, JCPDS Card No. 32-1129), except for a few weak peaks that probably originate from the impurities like MnO_2 and $Na_2Mn_3O_7$. Thus, the molar ratio of Na : Mn : Ti at 0.54 : 0.50 : 0.51 deviates from that of $Na_4Mn_4Ti_5O_{18}$ slightly. Although many combinations of reaction time, temperature and reactants have been explored, small quantities of impurities are still in the product, deserving the future studies on synthesis protocols. The Rietveld refinement of this pattern with the Highscore Plus programme is carried out based on the structure of $Na_4Mn_4Ti_5O_{18}$. As shown in Table S1 (ESI†), the lattice constants of the product are a = 9.1817(4) Å,

[a] *Key Laboratory of Colloid and Interface Chemistry, Ministry of Education School of Chemistry and Chemical Engineering, Shandong University, Jinan, 250100, P. R. China. E-mail: yangjian@sdu.edu.cn*
[b] *Hefei National Laboratory for Physical Science at Microscale, Department of Chemistry, University of Science and Technology of China, Hefei, 230026, P. R. China*

† Electronic supplementary information (ESI) available: The CV curves of NMTO nanorods between 2.0 and 4.7 V at a scan rate of 0.1 mV s^{-1}; the TEM image of NMTO/C nanorods; the Raman spectrum and TG curve of NMTO/C nanorods; the details of crystallographic data and Rietveld refinement of $Na_{0.54}Mn_{0.50}Ti_{0.51}O_2$. See DOI: 10.1039/c5cc02233a

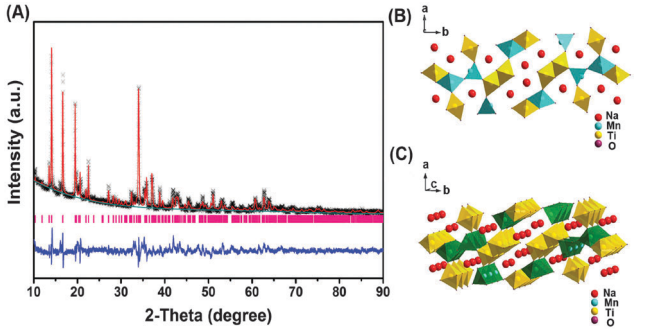

Fig. 1 (A) Observed (x) and Rietveld refined (red line) XRD pattern of $Na_{0.54}Mn_{0.50}Ti_{0.51}O_2$ (NMTO), Bragg positions (pink sticks) and the difference curve (blue line), (B) and (C) Crystal structures of $Na_{0.54}Mn_{0.50}Ti_{0.51}O_2$ isostructural with $Na_4Mn_4Ti_5O_{18}$.

b = 26.4451(5) Å, and c = 2.8746(7) Å. The good agreement between the experimental pattern and the calculated result confirms the isostructure of the product with $Na_4Mn_4Ti_5O_{18}$ (Fig. 1B), which is built by MO_5 square pyramids and MO_6 octahedra (M = Mn, Ti) *via* the vertex-sharing or edge-sharing connections. Interestingly, this construction of the polyhedrons results in two different tunnels, a large S-shaped tunnel and a small pentagon tunnel. Sodium ions in the large S-shaped tunnels are considered to be reversibly extracted,[11–13] while those in the small tunnels are fixed. Since the S-shaped tunnels are parallel to the *c*-axis (Fig. 1C), the short dimension along the *c*-axis would greatly benefit the quick insertion/extraction of sodium into the host material, improving the electrochemical kinetics. For the sake of clarity, the as-obtained $Na_{0.54}Mn_{0.50}Ti_{0.51}O_2$ in our case is denoted as NMTO from now on.

Fig. 2 shows the morphology of NMTO obtained by a modified molten-salt process. The resultant particles present a typical rod-like shape with diameters of 150–300 nm and lengths of 1–5 μm (Fig. 2A and B). To the best of our knowledge, this is the first time the size and shape control on NMTO are realized. Moreover, the involved synthesis is quite convenient, highly efficient and cost-effective. The resultant nanorods are straight, smooth and highly crystallized, as illustrated in Fig. 2C and D. The SAED pattern (Fig. 2C) not only demonstrates the single-crystal nature of the nanorods, but also indicates their growth direction perpendicular to the *c*-axis of $Na_4Mn_4Ti_5O_{18}$. The latter is particularly important for the sodium insertion/extraction in $Na_4Mn_4Ti_5O_{18}$, because their sodium-ion tunnnels are along the *c*-axis. Therefore, the small dimension along this direction in NMTO would shorten the diffusion distance of sodium and facilitate the sodium-transfer kinetics.

Fig. 3A illustrates the charge/discharge profiles of the NMTO nanorods at 0.2 C during the first three cycles. The cut-off voltages were set at a relatively narrow range, between 2.0 and 4.2 V, to assure the good cycling stability and inhibit the decomposition of the electrolyte (Fig. S1, ESI†). As a result, the NMTO nanorods give a charge/discharge capacity at 94/114 mA h g^{-1} for the 1st cycle. The following charge/discharge capacities in the 2nd and 3rd cycles are 124/113 and 123/113 mA h g^{-1}, respectively. The close charge and discharge capacities indicate a high coulombic efficiency upon cycling. The overlapped curves between the 2nd and 3rd cycles suggest the good cycling stability of the NMTO nanorods. These results are also supported by CV curves (Fig. 3B). There are two redox couples at 3.36/3.16 and 2.33/2.21 V, which could be attributed to the redox reactions of Mn^{3+}/Mn^{4+} and Mn^{2+}/Mn^{3+}.[18] The small voltage gap for each redox couple implies small polarization for the extraction and insertion of sodium in the NMTO nanorods.

The cycling performances of the NMTO nanorods are further examined at 0.2 and 1.0 C, as shown in Fig. 3C. They delivered a discharge capacity of 100 mA h g^{-1} after 150 cycles at 0.2 C (28 mA g^{-1}), or 67 mA h g^{-1} after 400 cycles at 1.0 C (140 mA g^{-1}), which corresponds to a capacity retention of ~88% or ~81%. The results are much better than those from the structural analogue reported by Zhou, $Na_{0.61}Mn_{0.52}Ti_{0.48}O_2$.[10] It showed a specific capacity of 70 mA h g^{-1} and a capacity retention of 81% after 100 cycles at 20 mA g^{-1} over 1.5–4 V. The significant

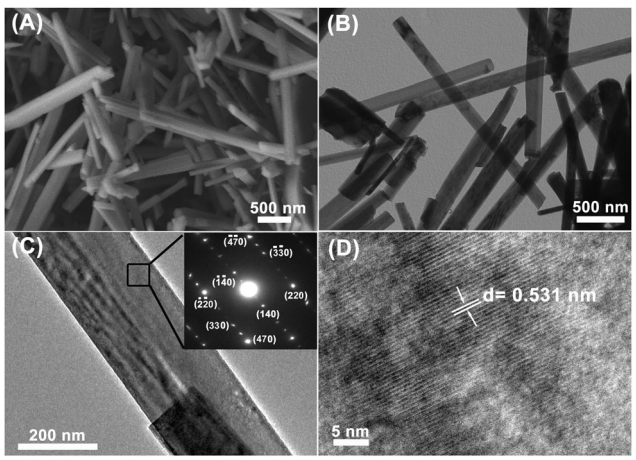

Fig. 2 (A) SEM, (B, C) TEM and (D) HRTEM images of NMTO nanorods. The inset of (C) is the SAED pattern of a single nanorod.

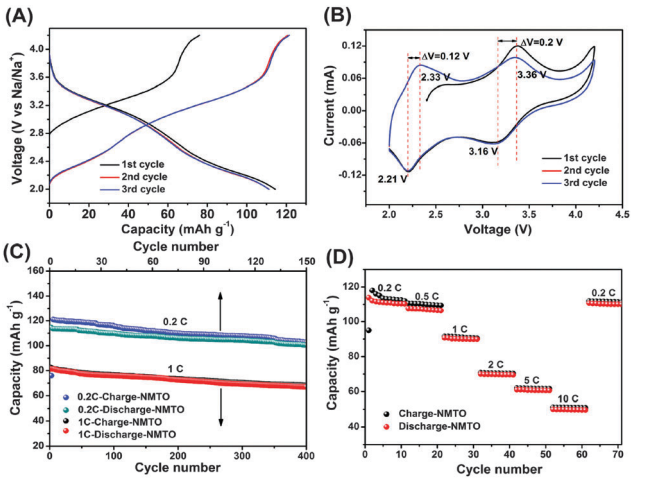

Fig. 3 Electrochemical properties of NMTO nanorods. (A) The charge/discharge profiles and (B) CV curves of NMTO nanorods for the first three cycles between 2.0 and 4.2 V; (C) cycling performances and (D) rate performances of NMTO nanorods between 2.0 and 4.2 V.

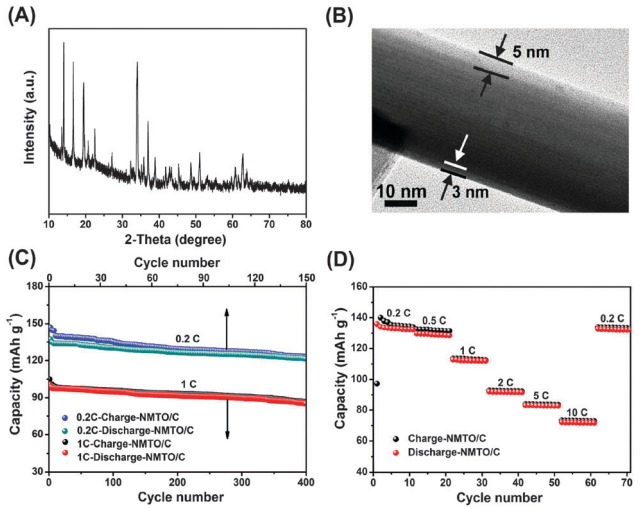

Fig. 4 (A) XRD pattern and (B) TEM image of the NMTO/C nanorods; (C) cycle performances and (D) rate performances of the NMTO/C nanorods between 2.0 and 4.2 V.

enhancement in our case could be associated with the appropriate combination of nanoscale size with well-defined shape, *i.e.* nanoscale size along the sodium diffusion channels in the NMTO nanorods. These results from the NMTO nanorods are also comparable to other Ti-based cathodes for SIBs. For example, $NaNi_{0.5}Ti_{0.5}O_2$ in an O3-type layer structure exhibited a capacity retention of 93% ($\sim$95 mA h g^{-1}) after 100 cycles at 20 mA g^{-1}, or 75% ($\sim$63 mA h g^{-1}) after 300 cycles at 100 mA g^{-1}.[7] Another Ti-containing cathode from Komaba's group,[8] $Na_{2/3}Ni_{1/3}Mn_{2/3-x}Ti_xO_2$ (x = 1/6) in a P2-type layer structure, reached a capacity of 110 mA h g^{-1} after 20 cycles at 0.05 C (12.1 mA g^{-1}), approximately 87% of the inital capacity. Singh *et al.* reported that the capacity retention of $NaFe_{0.2}Ni_{0.4}Ti_{0.4}O_2$ and $NaFe_{0.4}Ni_{0.3}Ti_{0.3}O_2$ could be improved by $NaClO_4$ and NaFSI based electrolytes to 72% and 64% after 75 cycles.[9]

Fig. 3D shows the rate capability of NMTO nanorods. As the rate increases from 0.2 C to 0.5, 1.0, 2.0 and 5.0 C, the reversible capacity could be kept at 111, 106, 90, 70, and 60 mA h g^{-1}. Even at a rate of 10 C, the capacity is still around 50 mA h g^{-1}. Most importantly, the capacity could be recovered, after the rate returns to 0.2 C. This result indicates the good electrochemical reversibility of the NMTO nanorods. Although the Jahn–Teller effect from Mn^{3+} ions is inevitably present in this cathode, NMTO nanorods still display high stability.

Surface coating of the NMTO nanorods by carbon is conducted to further improve their electrochemical performance. As shown in Fig. 4A, the diffraction positions and relative intensities of the peaks do not alter after the carbon coating, compared to the NMTO nanorods. A similar situation also occurs to their size and shape (Fig. S2, ESI†). But the high-resolution TEM image (Fig. 4B) on the edges of the nanorods clearly shows the formation of a carbon shell with a thickness of 3–5 nm, which would provide highly conductive channels for electron mobility between different NMTO nanorods. The formation of this carbon shell is also confirmed by the Raman spectra of the NMTO/C nanorods (Fig. S3A, ESI†). Thermogravimetric analysis further gives the carbon content of the NMTO/C nanorods at 18.8% (Fig. S3B, ESI†).

As expected, there is a significant improvement in their electrochemical properties, after the carbon coating. As shown in Fig. 4C, the NMTO/C nanorods exhibit a first discharge capacity of 137.3 mA h g^{-1} and retain the reversible capacity at 122 mA h g^{-1} after 150 cycles at a rate of 0.2 C, higher than those without carbon coating. Even at 1.0 C, the reversible capacity of the NMTO/C nanorods could be still preserved at 85 mA h g^{-1} after 400 cycles. The capacity retentions of the NMTO/C nanorods are 89% and 85% for 0.2 and 1 C respectively. Fig. 4D shows the rate capabilities of the NMTO/C nanorods. The reversible capacities are improved to 133, 129, 112, 92, 83 and 72 mA h g^{-1} at 0.2, 0.5, 1, 2, 5 and 10 C. When the rate returns to 0.2 C, the capacity could also be recovered, suggesting good reversibility. The enhanced kinetics is also reflected in the CV curves of the NMTO/C nanorods (Fig. S4, ESI†), which show small polarization in comparison to the NMTO nanorods.

In summary, tunnel-structured $Na_{0.54}Mn_{0.50}Ti_{0.51}O_2$ nanorods are successfully synthesized by a modified salt molten process. These nanorods present excellent electrochemical properties as a cathode material for sodium ion batteries, due to the proper combination of the nanoscale size, well-defined shape and tunnel structures. Their electrochemical performances could be further promoted by carbon coating on the surface to $\sim$122 mA h g^{-1} after 150 cycles at 0.2 C or $\sim$85 mA h g^{-1} after 400 cycles at 1 C. The simple, efficient and cost-effective synthesis and superior electrochemical performances of NMTO and NMTO/C nano-rods make them promising cathode materials for sodium ion batteries in the future.

This work is partially supported by 973 Project of China (No. 2011CB935901), National Nature Science Foundation of China (No. 91022033, 51172076 and 21471090), Shandong Provincial Natural Science Foundation for Distinguished Young Scholar (JQ201205), China Postdoctoral Science Foundation (No. 2014M561924), and start-up funding for new faculties in Shandong University.

Notes and references

1 Q. Q. Zhang, Q. C. Zhuang, S. D. Xu, X. Y. Qiu, Y. L. Cui, Y. L. Shi and Y. H. Qian, *Ionics*, 2012, **18**, 487.
2 Y. Wen, K. He, Y. J. Zhu, F. D. Han, Y. H. Xu, I. Matsuda, Y. Ishii, J. Cumings and C. S. Wang, *Nat. Commun.*, 2014, **5**, 4033.
3 L. W. Ji, M. Gu, Y. Y. Shao, X. L. Li, M. H. Engelhard, B. W. Arey, W. Wang, Z. M. Nie, J. Xiao, C. M. Wang, J. G. Zhang and J. Liu, *Adv. Mater.*, 2014, **26**, 2901.
4 Y. Liu, F. F. Fan, J. W. Wang, Y. Liu, H. L. Chen, K. L. Jungjohann, Y. H. Xu, Y. J. Zhou, D. Bigio, T. Zhu and C. S. Wang, *Nano Lett.*, 2014, **14**, 3445.
5 J. F. Qian, Y. Xiong, Y. L. Cao, X. P. Ai and H. X. Yang, *Nano Lett.*, 2014, **14**, 1865.
6 S. Li, J. X. Qiu, C. Lai, M. Ling, H. J. Zhao and S. Q. Zhang, *Nano Energy*, 2015, **12**, 224.
7 H. J. Yu, S. H. Guo, Y. B. Zhu, M. Ishidab and H. S. Zhou, *Chem. Commun.*, 2014, **50**, 457.
8 H. Yoshida, N. Yabuuchi, K. Kubota, I. Ikeuchi, A. Garsuch, M. Schulz-Dobrick and S. Komaba, *Chem. Commun.*, 2014, **50**, 3677.
9 G. Singh, F. Aguesse, L. Otaegui, E. Goikolea, E. Gonzalo, J. Segalini and T. Rojo, *J. Power Sources*, 2015, **273**, 333.
10 S. H. Guo, H. J. Yu, D. Q. Liu, W. Tian, X. Z. Liu, N. Hanada, M. Ishidab and H. S. Zhou, *Chem. Commun.*, 2014, **50**, 7998.

11 Y. Cao, L. Xiao, W. Wang, D. Choi, Z. Nie, J. Yu, L. V. Saraf, Z. Yang and J. Liu, *Adv. Mater.*, 2011, **23**, 3155.
12 D. Kim, S. Kang, M. Slater, S. Rood, J. T. Vaughey, N. Karan, M. Balasubramanian and C. S. Johnson, *Adv. Energy Mater.*, 2011, **1**, 333.
13 F. Sauvage, L. Laffont, J. M. Tarascon and E. Baudrin, *Inorg. Chem.*, 2007, **46**, 3289.
14 M. Zhao, Y. Fu, N. Xu, G. R. Li, M. T. Wu and X. P. Gao, *J. Mater. Chem. A*, 2014, **2**, 15070.
15 X. H. Rui, X. X. Zhao, Z. Y. Lu, H. T. Tan, D. H. Sim, H. H. Hng, R. Yazami, T. M. Lim and Q. Y. Yan, *ACS Nano*, 2013, **7**, 5637.
16 L. Wang, X. M. He, W. T. Sun, J. L. Wang, Y. D. Li and S. F. Fan, *Nano Lett.*, 2012, **12**, 5632.
17 B. Hai, A. K. Shukla, H. Duncan and G. Chen, *J. Mater. Chem. A*, 2013, **1**, 759.
18 R. Y. Chen, M. Knapp, M. Yavuz, R. Heinzmann, D. Wang, S. H. Ren, V. Trouillet, S. Lebedkin, S. Doyle, H. Hahn, H. Ehrenberg and S. Indris, *J. Phys. Chem. C*, 2014, **118**, 12608.